Cement & Concrete Composites 36 (2013) 116–120

Contents lists available at SciVerse ScienceDirect

Cement & Concrete Composites

journal homepage: www.elsevier.com/locate/cemconcomp

Micro-TiO_2 as a starting material for new photocatalytic tiles

C.L. Bianchi [a,b,*], S. Gatto [a], C. Pirola [a,b], M. Scavini [a], S. Vitali [a], V. Capucci [c]

[a] Università degli Studi di Milano, Dipartimento di Chimica, via C. Golgi, 19-20133 Milano, Italy
[b] Consorzio Interuniversitario Nazionale per la Scienza e Tecnologia dei Materiali, via G. Giusti, 9-50121 Firenze, Italy
[c] GranitiFiandre SpA, via Radici Nord, 112-42014 Castellarano, Italy

ARTICLE INFO

Article history:
Received 23 January 2012
Received in revised form 6 July 2012
Accepted 18 August 2012
Available online 3 September 2012

Keywords:
Photocatalytic tiles
Vitrified material
Micrometric TiO_2
NO_x
Methylene blue

ABSTRACT

New industrially produced photocatalytic tiles provide not only good photocatalytic performance, but also meet standard requirements with respect to hardness, lack of porosity, vitrified surface, durability. These characteristics were obtained mixing the photocatalytic materials with a commercial SiO_2-based compound conventionally used to create vitrified surfaces. In the preparation, a commercial micro-TiO_2 was used to avoid the use of traditional nanomaterials in powder form. Anatase form is maintained even after thermal treatments at 680 °C, as confirmed by both band gap and XRPD measurements on the final material. Photocatalytic degradation tests performed in water and air using methylene blue and NO_x as a model pollutant, respectively, confirm the good performance of the tiles in both liquid and gas phase.

1. Introduction

Market consumption of nanomaterials is growing. In the field of construction materials, nano-sized TiO_2 is particularly common since it has been traditionally used as a white pigment.

Nowadays TiO_2 is being used in air purification devices and as a surface treatment and additive in ceramics, cement, transportation infrastructure and glass. These products are being used or evaluated for their depollution, self-cleaning, antifungal, and environmental improvement attributes [1]. Incorporation of nanophotocatalysts into cementitious materials has been an important achievement in the field of photocatalytic pollution mitigation [2].

The increased presence of nanomaterials in commercial products has raised a growing public debate on whether the environmental and social costs of nanotechnologies outweigh their numerous benefits [3]. Up to now, few studies have investigated the toxicological and environmental effects of direct and indirect exposure to nanomaterials and nanoparticulate and no clear guidelines exist to quantify these effects [4].

Although TiO_2 is chemically inert, nanoTiO_2 can cause negative health effects. Investigations of Trouiller et al. found that TiO_2 nanoparticles can induce genotoxicity, oxidative DNA damage, and inflammation in a mice model [5].

There are no specific regulations on nanoparticles, except existing regulations covering the same material in bulk form [6]. Difficulties abound in devising such regulations, beyond self-imposed regulations by responsible companies, because of the likelihood of different properties exhibited by any type of nanomaterial, which are tunable by changing their size, shape and surface characteristics [7].

To avoid such possible drawbacks, in the present paper a new generation of photocatalytic tiles were prepared starting from a commercial micro-sized TiO_2 in the anatase form. Physical–chemical properties of the tiles were correlated with photoactivity results, obtained both in water and air using methylene blue and NO_x as a model pollutant, respectively, and fully discussed.

2. Experimental study

2.1. Preparation of vitrified tiles

Commercially available white tiles by GranitiFiandre SpA (White Ground Active®) were covered at the surface with a mixture of micro-TiO_2 (Kronos 1077) and a commercial SiO_2-based compound prepared via ball–mill. To achieve the desired product stability, at the end of the preparation procedure tiles were treated at high temperature (680 °C) for 80 min and then brushed to remove the powder present at the surface and that could alter the photocatalytic results (sample name: White Ground Active (WGA)). Temperature was precisely chosen to maintain the anatase form of the semiconductor and allow the vitrification of the tiles surface. Tiles were also prepared with the same procedure but without adding the photoactive oxide into the SiO_2-based compound for the sake of comparison (sample name White Ground (WG)).

* Corresponding author at: Università degli Studi di Milano, Dipartimento di Chimica, via C. Golgi, 19-20133 Milano, Italy.
E-mail addresses: claudia.bianchi@unimi.it (C.L. Bianchi), vcapucci@iris-group.it (V. Capucci).

0958-9465/$ - see front matter © 2012 Elsevier Ltd. All rights reserved.
http://dx.doi.org/10.1016/j.cemconcomp.2012.08.019

2.2. Sample characterization

Powder samples (micro-TiO_2 and micro-SiO_2-based compound) as well as photoactive and non-photoactive tiles were characterized by both surface and structural techniques.

XPS measurements were performed in an M-Probe Instrument (SSI) equipped with a monochromatic Al Kα source (1486.6 eV) with a spot size of 200 × 750 μm and a pass energy of 25 eV, providing a resolution for 0.74 eV. The surface area was investigated by nitrogen adsorption studies using the Brunauer–Emmett–Teller (BET) method. Measurements have been performed using a Sorptometer 1042 (Costech Instruments) at liquid nitrogen temperature (−196 °C).

Diffuse reflectance spectra of the powders were measured on UV–vis spectrophotometer (PerkinElmer, Lambda 35), which was equipped with a diffuse reflectance accessory, as reported previously [8].

The X-ray powder diffraction (XRPD) pattern at room temperature from the WGA powdered sample was collected at the high-resolution powder diffractometer at the ID31 beamline of the European Synchrotron Radiation Facility (ESRF), Grenoble, France [9]. A wavelength of $\lambda = 0.39620(9)$ Å was selected using a double-crystal Si(1 1 1) monochromator. The detector bank collected data in the $0 < 2\theta < 30°$ range. XRPD patterns were analyzed with the Rietveld method as implemented in the GSAS software suite of programs [10] which feature the graphical interface EXPGUI [11]. Line profiles were fitted using a modified pseudo-Voigt function [12] accounting for asymmetry correction [13].

SEM images were obtained using an electron microscopy Philips XL-30CP with RBS detector of back-scattered electrons. TEM images were obtained using a Philips 208 Transmission Electron Microscope.

2.3. Tiles testing procedures

Basic tiles features were verified after the coverage with the photocatalytic SiO_2-based mixture. Lack of porosity, resistance to surface abrasion and durability were measured by water absorption [14], rotation of an abrasive load on the tile surface [15] and determination of frost resistance (that is an intrinsic measurement of the product durability) [16], respectively.

Photocatalytic activity was evaluated both on tiles and powdered samples in water and air. In the former test, the degradation of methylene blue (10 μmol/l) was performed, accordingly with ISO 10678 procedure. For this purpose an aqueous solution was left in contact with the photocatalytic active surface under UV radiation (10 W/m^2), with light not capable of inducing the direct photolysis of the dye (320 nm $\leqslant \lambda \leqslant$ 400 nm), and with the overall result being the discoloration of the solution in 180 min. The amount of dye remaining in the solution was determined at regular intervals during the UV-radiation period using UV–vis spectroscopy. A reference measurement was either performed with the same sample without UV radiation or with an identical sample in a second container with the photoactive surface protected by a cover from the incident light beam. The results are used to calculate the specific degradation rate and the respective UV-radiation intensity efficiencies characteristic of the surface tested [17].

The specific degradation rate, R, is defined as:

$$R = \frac{\Delta A_\lambda V}{\Delta t \varepsilon d A}$$

where A_λ is the blue methylene absorbance, V the volume of the solution (cm^3), t the time (h) of reaction, ε the molar extinction coefficient (m^2/mol), d the length of the measurement cell (cm) and A is the irradiated area (cm^2).

NO_x degradation was performed in two plants working in two different experimental conditions: the first set-up, described elsewhere [18], working in static conditions, using a 20 W/m^2 iron halogenide lamp (Jelosil, model HG 500) emitting in the 315–400 nm wavelength range, photon flux 2.4×10^{-5} E dm^{-3} s^{-1}, checked by actinometry. The degradation was performed at different NO_x concentrations ranging from 40 ppb to 1000 ppb, room temperature, RH: 50%. The chosen values include the limit values reported on the Directive 2008/50/EC, in particular, 106.43 ppb (value not to be exceeded more than 18 times in a calendar year) and 212.96 ppb (alert threshold).

A second set-up was built following the ISO 22197-1 scheme and the test was performed in accordance with the rules of procedure (10 W/m^2, 1000 ppb NO_x, laminar flowing condition with a gas flow set at 180 l/min, RH: 50%). In both the experimental set-ups a chemiluminescence instrument was used to check the final conversion of the pollutant.

$$NO_x\ conversion = \frac{([NO_x]_{t=0} - [NO_x]_t)}{[NO_x]_{t=0}} \times 100$$

where $[NO_x]_{t=0}$ and $[NO_x]_t$ are the concentration at initial time and at a generic time t of reaction of NO_x, respectively.

3. Results and discussion

3.1. Characterization results

A TEM image of micro-TiO_2 is presented in Fig. 1. It is possible to observe that the commercial sample is composed by regular TiO_2 crystallites all in the micro-sized range and that no ultrafine particles are present [19].

A comparison between the features of micro-TiO_2 and micro-TiO_2+SiO_2-based compound after the calcination treatment at 680 °C is reported in Table 1.

On both samples XPS measurement reveals the presence of only Ti(IV) and a Ti/Si ratio of 0.15 for the micro-TiO_2+SiO_2-based compound.

As it can be observed in Table 1, the formulation with the SiO_2-based compounds and the following calcination step lead to a decrease of the surface area. For the same compounds the preservation of the pure anatase form was verified by both XRPD and XPS measurements. As reported by Anderson and Bard [20] the presence of SiO_2, together with TiO_2, enhances the formation of hydroxyl radical ·OH, which may be achieved via strong Brønsted acid sites at the TiO_2/SiO_2 interface region. Such incorporation inhibits the crystal growth of TiO_2 allowing the preservation of the anatase structure at high temperature [21].

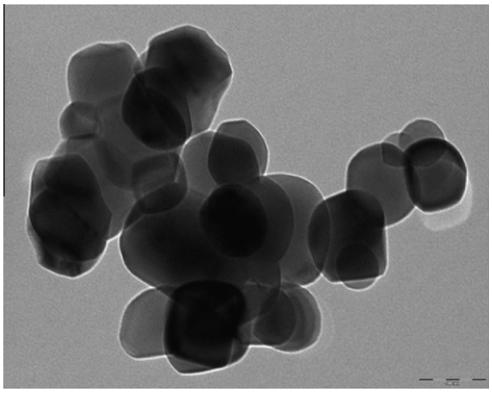

Fig. 1. TEM images of pure micro-sized commercial TiO_2.

Table 1
Physico-chemical features of both pure TiO_2 (Kronos 1077) and after its formulation and calcination at 680 °C with the SiO_2-based compound.

Sample	BET surface area (m^2/g)	XRPD	XPS Ti $2p_{3/2}$ (eV)	UV–vis (eV)
Pure TiO_2	11.0	Pure anatase	458.5	3.22
TiO_2+SiO_2-based compound	2.6	Pure anatase	458.4	3.23

In Fig. 2 the XRPD pattern of the sample is shown. The experimental (crosses) and calculated (continuous line) curves are reported together with the difference curve (bottom). The XRPD pattern of the sample is correctly interpreted using a single crystalline phase, which is the anatase TiO_2 polymorph: space group $I4_1/amd$ (N°141, origin choice 2). In this structure Ti ions lie in (0, 1/4, 3/8) site while O in (0, 1/4, z) [22]. The refined structural parameters are shown in Table 2. The nearest neighbors Ti–O distances are the following: d(Ti–O) × 4 → 1.9354(2) Å; d(Ti–O) × 2 → 1.9734(9) Å.

The image of the WGA photoactive tile (Fig. 3b) shows a quite homogeneous surface with a good distribution of both Si and Ti atoms, as revealed by EDX analysis. As expected, no Ti signals were observed on the non-photoactive tile (Fig. 3a).

3.2. Tiles physical properties

A fundamental aspect of the new photoactive tiles is the preservation of the basic tiles features such as lack of porosity, hardness and durability. For this reason all these features were carefully checked.

Lack of porosity was measured by water absorption. Water absorption rates are a measurement of how much moisture a specific type of porcelain tile may absorb on an ongoing basis. Some types of tile may crack if the moisture penetration is too high. In our case a porosity value of less than 0.5% was obtained for both WGA and WG samples allowing to classify both the tile as impervious (extremely dense) and categorized them as porcelain tiles.

Tiles hardness was verified by the measure of the resistance to abrasion which involves the rotation of a defined abrasive powder load on the surface of a tile sample for a specific number of revolutions, and assigning the tile to a PEI class of abrasion resistance on the basis of a visual examination of the abraded test samples under well-defined conditions of observations, in agreement with the recommendations of the CEC (Federation Europenne des Fabricants de Carreaux Ceramiques) [15]. In our case both WG and WGA were classified as PEI IV that means that they are suitable for use in areas subjected to considerable traffic with the presence of some abrasive dirt.

Tiles durability was checked verifying their resistance to frost. After impregnation with water, the tiles were subjected to temperature cycles between +5 and −5 °C, during a minimum of 100 freeze–thaw cycles. No evident cracks or damages were observed on our samples.

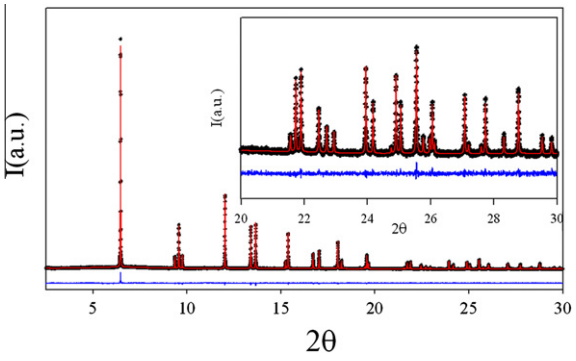

Fig. 2. XRPD pattern of WGA powdered sample. Measured (black crosses) and calculated (red line) profiles are shown as well as residuals (blue line). The inset highlights the high angle 2θ region. (For interpretation of the references to color in this figure legend, the reader is referred to the web version of this article.)

Table 2
Rietveld refinement results referring to TiO_2 sample.

Space group	$I4_1/amd$
a (Å)	3.78550
c (Å)	9.51000
V (Å^3)	136.278
z_O	0.1675
U_{Ti} (Å^2)	0.0042
U_O (Å^2)	0.0047
wRp	0.073
Rp	0.056
χ^2	1.29
$R(F^2)$	0.038

3.3. Photocatalytic test

The degradation of methylene blue in water was monitored for a reaction time of 3 h. The discoloration of the solution was visible with naked eye and a final conversion value of 22.5% was calculated for WGA, compared with a 1.8% achieved by the non-photocatalytic tile WG.

In the gas phase (air) a modest result was observed for the NO_x degradation (NO_x is a generic term for mono-nitrogen oxides NO and NO_2) using the continuous reactor, strictly built following the ISO 22197-1 specifications. Due to the lack of porosity of the tested tiles (mentioned above) together with the velocity of the gas (contact time 0.4 s), the adsorption of the pollutant molecules at the sample surface cannot occur, so preventing the photocatalytic process. As the contact time is the time passed by the reactants in contact with the catalytic active sites, a very short contact time requires a high active surface, mainly able to adsorb quickly the reactant before acting as a catalyst. In our case, the vitrified surface does not allow a sufficiently rapid adsorption of the pollutant molecule and thus an inefficacy of the subsequent photocatalytic process. This result highlights the ineffectiveness of the standard ISO 22197-1 procedure to test the photocatalytic efficiency on vitrified, non-porous, materials [23].

On the contrary, good results were obtained testing WGA in the gas phase but in static conditions. In this case, using 1000 ppb of NO_x, i.e. the same amount required by the ISO 22197-1 specifications, the 53% of degradation was measured after 6 h.

A very interesting trend (Fig. 4) was observed following the NO_2 degradation at different pollutant concentration. More in detail, the tests were carried out the material with 106 ppb (value not to be exceeded more than 18 times in a calendar year), and 212 ppb (alert threshold), according to the Directive 2008/50/EC of the European Parliament and stating the guidelines for the protection of the human health.

NO_2 was chosen as specific reference pollutant instead of the more generic NO_x, because of its higher hazardousness. NO_2 is in fact an irritant agent affecting the mucosa of the eyes, nose, throat, and respiratory tract and the continued exposure to high NO_2 levels can contribute to the development of acute or chronic bronchitis [24].

It is possible to observe (Fig. 4) that, as the amount of starting pollutant is decreased, the time necessary to bring its concentration under the limit required by the European Directive (21 ppb)

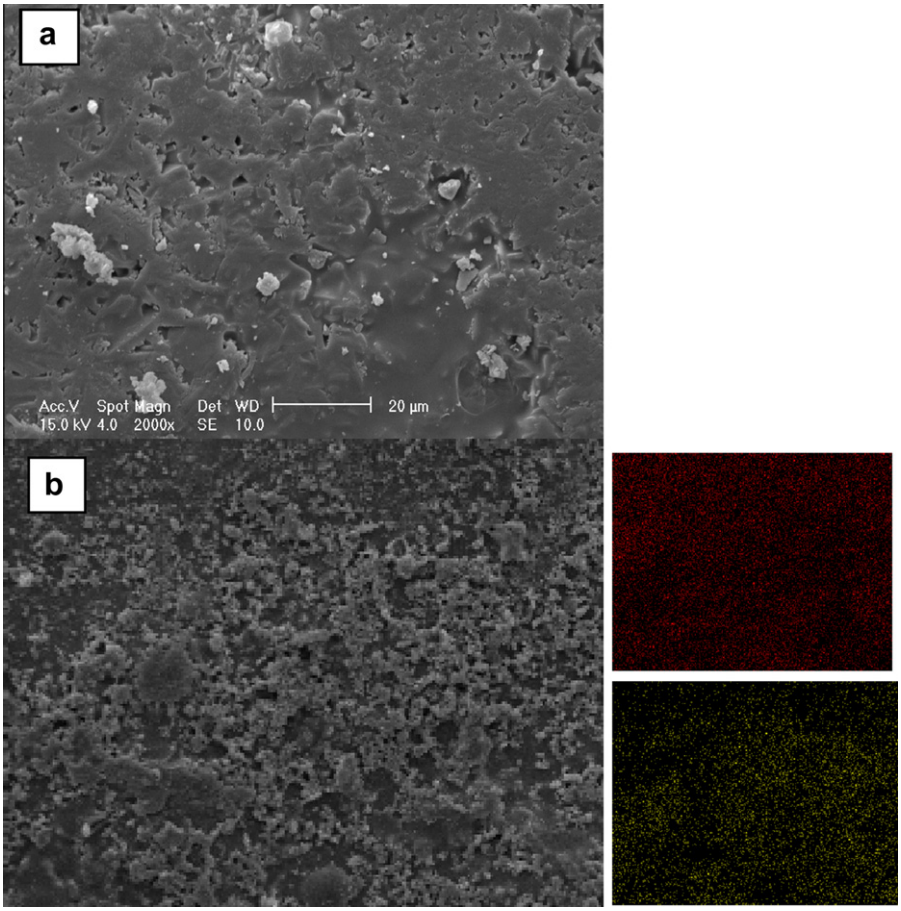

Fig. 3. SEM images (2000×) of WG tile (a), and photocatalytic WGA (b). Element mapping by EDX for WGA sample (red picture: Si; green picture: Ti). (For interpretation of the references to color in this figure legend, the reader is referred to the web version of this article.)

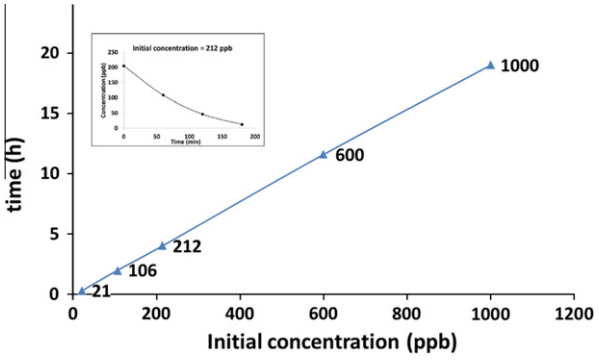

Fig. 4. Time necessary to degrade the pollutant and decrease its amount under the limit value required by the Directive 2008/50/EC of the European Parliament and of the council on ambient air quality and cleaner air for Europe (21 ppb); 20 W/m^2, RH 50%, static conditions.

also decreases. In the Fig. 4 inset, the degradation trend can be observed in the case of an initial pollutant concentration close to the alert threshold.

Therefore, it is possible to conclude that, under real pollution conditions, simulating a day in the absence of wind (static conditions) WGA is able to degrade NO_2 in a very efficient way bringing the pollutant concentration down to the required limit (21 ppb) in a matter of hours.

4. Conclusions

In the present paper the photocatalytic activity of vitrified tiles is discussed. To avoid possible future drawbacks due to the nanometric size of the photocatalytic active powder, the samples were prepared using a commercial micro-sized TiO_2.

The final tile couples the classical requested features typical for a tile (hardness, lack of porosity, vitrified surface, durability) with good performance as photocatalytic material both in water and in air. White Ground Active tiles (WGA) show good photocatalytic performances especially in the pollution ranges indicated by the Directive 2008/50/EC of the European Parliament and of the Council on ambient air quality and cleaner air for Europe (NO_2 concentration lower than 200 µg/m^3, corresponding to 106.43 ppb).

A final remark is devoted to the inadequacy of the ISO 22197-1 specifications as standard test on vitrified, non-porous materials. In fact, due to the lack of porosity of the tested tiles together with the velocity of the gas (contact time 0.4 s), the adsorption of the pollutant molecules at the sample surface cannot occur, so preventing the photocatalytic process.

Acknowledgments

The authors gratefully acknowledge the European Synchrotron Radiation Facility for provision of beam time and Dr. Caroline Curfs for assistance in using the ID31 beamline.

References

[1] Maltby JE, Geninazza E. Photocatalytic products for the construction industry. In: Proceedings of 30th FATIPEC congress, vol. 2; 2010. p. 798–07.
[2] Chen J, Poon CS. Hydration and properties of nano-TiO_2 blended cement composites. Environ Sci Technol 2009;43(23):8948–52.
[3] Colvin VL. The potential environmental impact of engineered nanomaterials. Nat Biotechnol 2003;21(10):1166–70.
[4] Hye Won K, Eun-Kyung A, Bo Keun J, Hyoung-Kyu Y, Kweon Haeng L, Young L. Nanoparticulate-induced toxicityand related mechanism in vitro and in vivo. J Nanoparticle Res 2009;11:55–65.
[5] Trouiller B, Reliene R, Westbrook A, Solaimani P, Schiestl RH. Titanium dioxide nanoparticles induce DNA damage and genetic instability in vivo in mice. Cancer Res 2009;69:8784–9.
[6] Bowman DM, Hodge GA. A small matter of regulation: an international review of nanotechnology regulation. Columbia Sci Technol Law Rev 2007;8(1).
[7] Albrecht MA, Cameron WE, Raston CL. Green chemistry and the health implications of nanoparticles. Green Chem 2006;8:417–32.
[8] Bianchi CL, Cappelletti G, Ardizzone S, Gialanella S, Naldoni A, Oliva C, et al. N-doped TiO_2 from $TiCl_3$ for photodegradation of air pollutants. Catal Today 2009;144:31–6.
[9] Fitch AN. The high resolution powder diffraction beam line at ESFR. J Res Natl Inst Stand Technol 2004;109:133–42.
[10] Larson AC, Von Dreele RB. General structural analysis system (GSAS). Los Alamos National Laboratory Report LAUR; 2004. p. 86–748.
[11] Toby BH. EXPGUI, a graphical user interface for GSAS. J Appl Cryst 2001;34:210–4.
[12] Thompson P, Cox DE, Hastings JB. Rietveld refinement of Debye-Scherrer synchrotron X-ray data from alumina. J Appl Crystallogr 1987;20:79–83.
[13] Finger LW, Cox DE, Jephcoat AP. A correction for powder diffraction peak asymmetry due to axial divergence. J Appl Crystallogr 1994;27:892–900.
[14] ASTM C373-88(2006). Standard test method for water absorption, bulk density, apparent porosity, and apparent specific gravity of fired whiteware products. West Conshohocken (PA): ASTM International; 2003. http://dx.doi.org/10.1520/C0033-03, <www.astm.org>.
[15] ISO 10545-7. Ceramic tiles – Part 7: Determination of resistance to surface abrasion for glazed tiles; 1996. <www.iso.org>.
[16] ISO 10545-12. Determination of frost resistance. <www.iso.org>.
[17] ISO 10678. Determination of photocatalytic activity of surfaces in an aqueous medium by degradation of methylene blue. <www.iso.org>.
[18] Ardizzone S, Bianchi CL, Cappelletti G, Gialanella S, Pirola C, Ragaini V. Tailored anatase/brookite nanocristalline TiO_2. The optimal particle features for liquid-and-gas-phase photocatalytic reactions. J Phys Chem C 2007;111:13222–31.
[19] http://nl-int.com/khome.nsf/Complete_Typelist.pdf.
[20] Anderson C, Bard A. Improved photocatalytic activity and characterization of mixed TiO_2/SiO_2 and TiO_2/Al_2O_3 materials. J Phys Chem B 1997;101:2611–6.
[21] Xie TH, Lin J. Origin of photocatalytic deactivation of TiO_2 film coated on ceramic substrates. J Phys Chem C 2007;111:9968–74.
[22] Howards CJ, Sabine TM, Dickson F. Structural and thermal parameters for rutile and anatase. Acta Cryst B 1991;47:462–8.
[23] Bianchi CL, Pirola C, Gatto S, Nucci S, Minguzzi A, Cerrato G, Biella S, Capucci V. New surface properties in porcelain gres tiles with a look to human and environmental safety. Adv Mater Sci Eng 2012;2012:970182(8 pp.). http://doi:10.1155/2012/970182.
[24] http://www.epa.gov/iaq/no2.html.